Synthesis, spectral and molecular studies of half-sandwich arene ruthenium and Cp*Rh/Cp*Ir complexes containing bidentate P-N and E–N ligands (E = S, Se) based on diphenyl(2-pyridyl)phosphine

Mahesh Kalidasan, R. Nagarajaprakash & Kollipara Mohan Rao

Taylor & Francis
Taylor & Francis Group

Synthesis, spectral and molecular studies of half-sandwich arene ruthenium and Cp*Rh/Cp*Ir complexes containing bidentate P-N and E–N ligands (E = S, Se) based on diphenyl (2-pyridyl)phosphine

MAHESH KALIDASAN†, R. NAGARAJAPRAKASH‡ and
KOLLIPARA MOHAN RAO*†

†Department of Chemistry, North Eastern Hill University, Shillong, India
‡Department of Chemistry, Pondicherry University, Puducherry, India

The chalcogenide ligands {E=PPh$_2$Py} (E = O, S, Se) were prepared by direct oxidation of diphenyl (2-pyridyl)phosphine using H$_2$O$_2$, S, and Se powder, respectively. The reaction of ligand with starting metal precursors [(arene)RuCl$_2$]$_2$ {M = Ru, arene = benzene; *p*-cymene} and [Cp*MCl$_2$]$_2$ (M = Rh, Ir) afforded a series of cationic half-sandwich complexes, [(arene/Cp*)MCl{κ^2-(*NE*)-EPPh$_2$Py)}]$^+$. Reaction of O=PPh$_2$Py 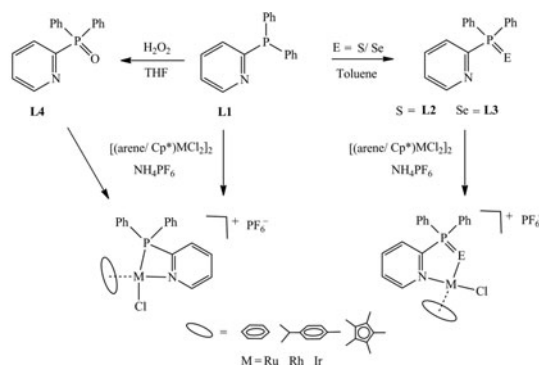with precursors yielded known complexes [(arene/Cp*)MCl {κ^2-(*PN*)-PPh$_2$Py)}]$^+$ instead of expected complexes [(arene/Cp*)MCl{κ^2-(*NO*)-O=PPh$_2$Py)}]$^+$. All new complexes were isolated as PF$_6^-$ counterion and characterized by spectroscopic techniques like FT-IR, NMR, mass, and UV–vis. Some representative complexes were structurally determined by X-ray crystallographic analysis, revealing typical three-legged piano stool geometry around the metal center with a five-membered metallacycle.

Keywords: Arene ligands; Ruthenium; Rhodium; Iridium; Diphenyl(2-pyridyl)phosphine ligands

---

*Corresponding author. Emails: mohanrao59@gmail.com; kmrao@nehu.ac.in

1. Introduction

The heterobidentate P,N-donor diphenyl(2-pyridyl)phosphine (PPh$_2$Py) represents an important class of hemilabile ligands which binds to metal with medium strength. Metal complexes containing hemilabile ligands provided a potential site for the reversible binding to metal center because of their dynamic chelating ability. Owing to their ability to reversibly bind, hemilabile metal complexes are extremely important in catalysis and have been used in various organic transformations [1–3].

Organophosphine ligands having S or Se donors receive attention due to their catalytic properties [4, 5]. A number of transition metal complexes containing functionalized P-X (X = chalcogen donors) ligands have been reported. We became interested in the study of E=PPh$_2$Py as potentially hemilabile ligands and their catalytic studies. For example, rhodium and ruthenium carbonyl complexes of functionalized phosphine chalcogen donors, P-X (X = O, S, Se), have been studied in catalytic applications particularly in carbonylation of alcohols, hydrogenation of unsaturated substrates, and hydroformylation of alkenes for industrially important organic molecules [6–10].

Our group has been interested in the synthesis of arene ruthenium and Cp*Rh/Cp*Ir complexes with various mono/bidentate ligands containing nitrogen donors. Recently, we reported the synthesis of neutral and cationic half-sandwich platinum group complexes with diphenyl(2-pyridyl)phosphine [11–13]. However, arene ruthenium and Cp*Rh/Cp*Ir complexes with chalcogenide, E=PPh$_2$Py (E = S, Se), have not been explored. As a part of our continuing study, we would like to report syntheses of a series of new mononuclear half-sandwich complexes of arene Ru(II), Cp*Rh(III), and Cp*Ir(III) with bidentate phosphine chalcogenide ligands.

2. Experimental

2.1. *Physical methods and materials*

All the experiments were performed under normal conditions. All reagents were purchased from commercial sources and used as received. RuCl$_3$·nH$_2$O, RhCl$_3$·nH$_2$O, and IrCl$_3$·nH$_2$O were purchased from Arora Matthey limited; diphenyl(2-pyridyl)phosphine was obtained from Aldrich; sulfur and selenium powder were acquired from Merck. The solvents were purified and dried according to standard procedures [14]. The starting metal precursors [(benzene)RuCl$_2$]$_2$, [(p-cymene)RuCl$_2$]$_2$ and [Cp*MCl$_2$]$_2$ (M = Rh or Ir) [15], chalcogenide E=PPh$_2$Py were prepared by modified literature methods [5]. NMR spectra were recorded on a Bruker Avance II 400 MHz spectrometer. Infrared spectra were recorded as KBr pellets on a Perkin-Elmer 983 spectrophotometer. Elemental analyses were obtained on a Perkin-Elmer 2400 CH/N analyzer. Mass spectra were obtained using a Waters ZQ 4000 mass spectrometer by the ESI method in positive mode. Absorption spectra were obtained at room temperature using a Perkin-Elmer Lambda 25 UV/visible spectrophotometer.

2.2. *Single-crystal X-ray structures analyses*

Orange or yellow crystals of **2**, **6–9**, and **12** were obtained by slow diffusion of hexane into acetone solution of the corresponding complexes. Single-crystal X-ray diffraction

Table 1. Crystallographic and structure refinement parameters for complexes.

	2	6	7	8	9	12. H₂O
Empirical formula	$C_{27}H_{28}ClF_6NP_2RuS$	$C_{27}H_{28}ClF_6NP_2RuSe$	$C_{27}H_{29}ClF_6NP_2RhSe$	$C_{27}H_{29}ClF_6IrNP_2Se$	$C_{23}H_{20}ClF_6NP_2Ru$	$C_{27}H_{29}ClF_6IrNOP_2$
Formula weight	711.02	757.92	760.77	850.06	622.86	789.12
Temperature (K)	292.5(3)	291.77(12)	293(2)	293(2)	291.59(18)	290.6(2)
Wavelength (Å)	0.71073 Å	0.71073	0.71073	0.71073	0.71073	0.71073
Crystal system, space group	Monoclinic, $P2_1/n$	Monoclinic, $P2_1/n$	Triclinic, $P\bar{1}$	Triclinic, $P\bar{1}$	Monoclinic, $P2_1/n$	Monoclinic, $P2_1/c$
Unit cell dimensions	$a = 11.1428(2)$Å $\alpha = 90°$ $b = 15.3394(3)$Å $\beta = 92.528(17)°$ $c = 17.4201(3)$Å $\pi = 90°$	$a = 11.2530(3)$Å $\alpha = 90°$ $b = 15.3439(6)$Å $\beta = 93.267(3)°$ $c = 17.3956(5)$Å $\pi = 90°$	$a = 8.6448(4)$Å $\alpha = 98.170(5)°$ $b = 11.3839(9)$Å $\beta = 97.718(4)°$ $c = 15.5573(7)$Å $\pi = 100.918(5)°$	$a = 8.7145(4)$Å $\alpha = 98.245(3)°$ $b = 11.3780(5)$Å $\beta = 97.406(3)°$ $c = 15.6374(5)$Å $\pi = 100.845(3)°$	$a = 11.1146(4)$ A $\alpha = 90°$ $b = 15.8780(4)$ A $\beta = 91.261(3)°$ $c = 13.8150(3)$ A $\pi = 90°$	$a = 11.9797(3)$Å $\alpha = 90°$ $b = 7.9851(16)$Å $\beta = 96.924(2)°$ $c = 30.6201(6)$Å $\pi = 90°$
Volume (Å³)	2974.63(10)	2998.74(17)	1467.43(15)	1487.56(10)	2437.46(12)	2907.73(12)
Z, Calculated density (Mg m⁻³)	4, 1.588	4, 1.679	2, 1.722	2, 1.898	4, 1.701	4, 1.798
Absorption coefficient (mm⁻¹)	0.851	1.988	2.079	5.965	1.000	4.855
F(0 0 0)	1432	1512	756	820	1240	1536
Crystal size (mm)	$0.25 \times 0.22 \times 0.13$	$0.15 \times 0.12 \times 0.08$	$0.25 \times 0.21 \times 0.18$	$0.28 \times 0.28 \times 0.28$	$0.21 \times 0.21 \times 0.12$	$0.29 \times 0.25 \times 0.19$
Theta range for data collection	3.455–28.352°	3.625–27.83°	3.969–28.462°	3.711–28.216°	3.422–28.336°	3.934–28.407°
Limiting indices	$-13 <= h <= 12$, $-19 <= k <= 19$, $-22 <= l <= 21$	$-14 <= h <= 14$, $-20 <= k <= 11$, $-22 <= l <= 11$	$-10 <= h <= 11$, $-15 <= k <= 13$, $-20 <= l <= 20$	$-10 <= h <= 11$, $-13 <= k <= 15$, $-20 <= l <= 18$	$-14 <= h <= 14$, $-20 <= k <= 20$, $-8 <= l <= 18$	$-11 <= h <= 14$, $-9 <= k <= 9$, $-36 <= l <= 24$
Absorption correction	Multi-scan	Multi-scan	Multi-scan	Multi-scan	Multi-scan	Multi-scan
Reflections collected/ unique	13,287/5185 [R(int) = 0.0272]	13,347/5131 [R(int) = 0.0287]	12,213/5691 [R(int) = 0.0212]	12,202/5711 [R(int) = 0.0389]	11,100/4657 [R(int) = 0.0207]	12,297/4790 [R(int) = 0.0231]
Completeness to $\theta = 25.242$	99.8%	99.8%	99.7%	99.8%	99.7%	99.8%
Data/restraints/ parameters	6799/0/352	6784/0/349	6722/0/352	6722/0/345	5533/0/308	5112/0/357
Goodness-of-fit on F^2	1.019	1.027	1.043	1.052	1.102	1.299
Final R indices [$I > 2\sigma (I)$]	R1 = 0.0456, wR2 = 0.1094	R1 = 0.0451, wR2 = 0.1054	R1 = 0.0382, wR2 = 0.0982	R1 = 0.0427, wR2 = 0.1016	R1 = 0.0654, wR2 = 0.1720	R1 = 0.0392, wR2 = 0.0705
R indices (all data)	R1 = 0.0659, wR2 = 0.1223	R1 = 0.0677, wR2 = 0.1183	R1 = 0.0487, wR2 = 0.1057	R1 = 0.0550, wR2 = 0.1085	R1 = 0.0767, wR2 = 0.1820	R1 = 0.0431, wR2 = 0.0716
Largest diff. peak and hole (e A⁻³)	0.736 and −0.582	0.953 and −0.860	1.085 and −0.725	1.667 and −1.365	3.841 and −0.831	1.688 and −1.145

Table 2. Selected bond lengths (Å) and angles (°) of **2**, **6–9**, and **12**.

Complex	**2**	**6**	**7**	**8**	**9**	**12**
M(1)–P(1)	–	–	–	–	2.3208(12)	2.3113(13)
M(1)–E(1)	2.4094(9)	2.5185(5)	2.5201(5)	2.5189(7)	–	–
M(1)–N(1)	2.123(3)	2.127(3)	2.125(3)	2.109(5)	2.118(4)	2.150(5)
M(1)–Cl(1)	2.3815(12)	2.3867(13)	2.3924(9)	2.4034(17)	2.3860(13)	2.3944(14)
P(1)–E(1)	1.9819(13)	2.1384(11)	2.1329(9)	2.1463(16)	–	–
M(1)–C_{ave}	2.191(4)	2.196(4)	2.158(4)	2.166(7)	2.193(7)	2.184(5)
M(1)–CNT	1.677	1.683	1.788	1.796	1.699	1.810
N(1)–M(1)–P(1)/E(1)	86.25(9)	86.87(9)	87.30(7)	87.98(13)	66.97(12)	66.89(12)
P(1)/E(1)–M(1)–Cl(1)	85.27(4)	85.25(4)	89.81(3)	87.32(5)	88.54(4)	89.65(5)
N(1)–M(1)–Cl(1)	82.70(9)	83.40(10)	85.45(8)	83.95(14)	82.37(12)	82.45(12)

Notes: CNT represents the centroid of the arene/Cp* ring; C_{ave} represents the average bond distance centroid of the arene/Cp* ring carbon and metal atom.

measurements were carried out on an Oxford Diffraction Xcalibur Eos Gemini diffractometer. Crystal data were collected at 300 K using graphite monochromated Mo Kα radiation (λ = 0.71073 Å). The strategy for data collection was evaluated using the CrysAlisPro CCD software. Crystal data were collected by standard "phi-omega scan" techniques and were scaled and reduced using CrysAlisPro RED software. The structures were solved by direct methods using SHELXS-97 and refined by full-matrix least-squares with SHELXL-97 refining on F^2 [16, 17]. The positions of all atoms were obtained by direct methods. All non-hydrogen atoms were refined anisotropically. Hydrogens were placed in geometrically constrained positions and refined with isotropic temperature factors, generally 1.2 Ueq of their parent atoms. Crystallographic details are summarized in table 1 and selected bond lengths and angles are presented in table 2. Figures 1–3 were drawn with ORTEP-3 and figure 4 was drawn with MERCURY [18].
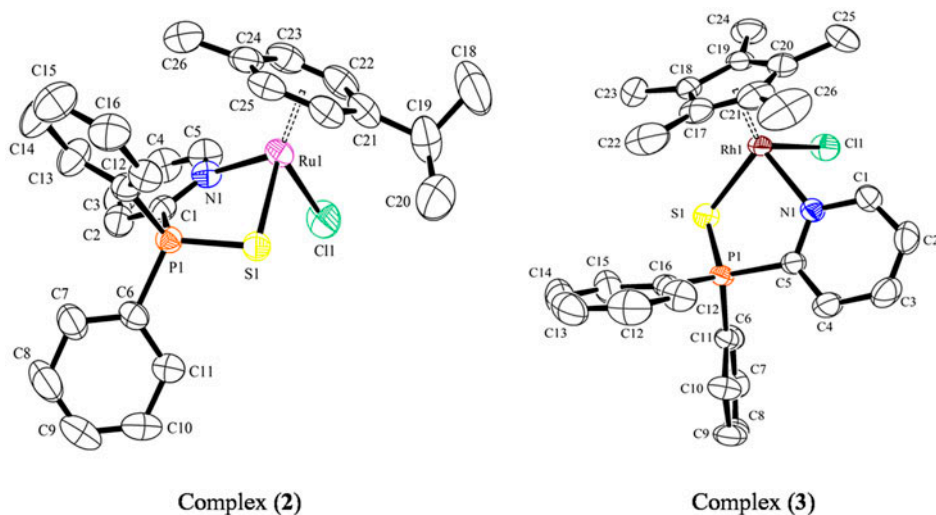

Figure 1. Molecular structures of [(p-cymene)Ru(S=PPh$_2$Py)Cl]PF$_6$ (**2**) and [Cp*Rh(S=PPh$_2$Py)Cl]PF$_6$ (**3**) with 50% probability thermal ellipsoids. Counterion and hydrogens are omitted for clarity.

2.3. *Syntheses of metal complexes (1–8)*

Mixture of the metal precursor [(arene)RuCl$_2$]$_2$ or [Cp*MCl$_2$]$_2$ (0.1 mmol) and E=PPh$_2$Py (E = S, Se) (0.2 mmol) was dissolved in methanol (20 mL) then stirred at room temperature for 6 h. A yellow or orange precipitate formed immediately after adding NH$_4$PF$_6$ (2 molar equivalents) to the reaction mixture. The precipitate was washed with methanol (5 mL), diethyl ether (3 × 10 mL) and dried under vacuum.

2.3.1. [(Benzene)Ru(S=PPh$_2$Py)Cl]PF$_6$ (1). Color: orange precipitate; yield: 50 mg (77%); IR (KBr, cm^{-1}): 3449(b), 3090(m), 1628(w), 1587(m), 1481(w), 1451(m), 1437(s), 1383(m), 1335(w), 1309(m), 1286(w), 1187(m), 1131(w), 1102(s), 1023(m), 993(w), 840 (vs), 766(s), 742(s), 711(m), 693(s), 558(s), 525(s), 510(s); ^{1}H NMR (400 MHz, CD$_3$CN): δ = 9.20 (d, 1H, H$_{JJ}$ = 3.25, py ring), 7.84 (t, 1H, py ring), 7.71–7.61 (m, 3H, py & ph ring), 7.58–7.54 (m, 4H, ph ring), 7.38–7.30 (m, 4H, ph ring), 7.15 (t, 1H, py ring), 5.31 (s, 6H, benzene ring); ^{13}C NMR (400 MHz, CD$_3$CN): δ = 160.28, 154.53, 139.61, 134.71, 132.91, 132.01, 130.74, 129.82, 128.69, 86.20; ESI-MS: 509.90 [M$^+$] peak, 475.03 [M$^+$–Cl] peak, 214.89 [(ben)RuCl$^+$] peak; UV–vis {CH$_3$CN, λ_{max} nm (ε, M^{-1} cm^{-1})}: 226 (5800), 330(500); Anal. Calcd for C$_{23}$H$_{20}$NSRuClPF$_6$ (654.96) (%): C, 42.18; H, 3.08; N, 2.12. Found (%): C, 42.50; H, 3.22; N, 2.20.

2.3.2. [(p-Cymene)Ru(S = PPh$_2$P)Cl]PF$_6$ (2). Color: orange precipitate; yield: 57 mg (80%); IR (KBr, cm^{-1}): 3449(b), 3080(m), 2969(m), 1629(w), 1587(m), 1483(m), 1437(s), 1383(w), 1333(w), 1283(m), 1129(w), 1101(s), 1058(m), 1028(w), 998(m), 839(vs), 768(s), 741(s), 710(s), 693(s), 557(vs), 525(s), 509(s); ^{1}H NMR (400 MHz, CD$_3$CN): δ = 9.38 (d, 1H, H$_{JJ}$ = 3.25, py ring), 8.10 (t, 1H, py ring), 7.98–7.92 (m, 3H, py & ph ring), 7.81–7.77 (m, 4H, ph ring), 7.62–7.51 (m, 4H, ph ring), 5.86 (d, 2H, H$_{JJ}$ = 3.75, ph ring), 5.63 (d, 2H, H$_{JJ}$ = 3.75, ph ring), 2.70 (sep, 1H, Ar$_{(p\text{-}Cy)}$), 2.48 (s, 3H, CH$_3$), 1.99 (s, 3H, CH$_3$Ar$_{(p\text{-}Cy)}$), 1.32 (d, 6H, H$_{JJ}$ = 4.00, CH$_3$Ar$_{(p\text{-}Cy)}$), 1.21 (d, 6H, H$_{JJ}$ = 4.25, CH$_3$Ar$_{(p\text{-}Cy)}$); ^{13}C NMR (400 MHz, CD$_3$CN): δ = 159.64, 154.55, 139.71, 134.68, 132.85, 132.10, 130.78, 129.87, 129.02, 103.16, 90.59, 85.04, 83.67, 30.49, 21.76, 16.98; ESI-MS: 566.10 [M$^+$] peak, 531.01 [M$^+$–Cl] peak, 236.05 [(p-cy)RuCl$^+$] peak; UV–vis {CH$_3$CN, λ_{max} nm (ε, M^{-1} cm^{-1})}: 229(6600), 335(600); Anal. Calcd for C$_{27}$H$_{28}$NSRuClPF$_6$ (711.04) (%): C, 45.61; H, 3.97; N, 1.97. Found (%): C, 45.73; H, 4.17; N, 2.10.

2.3.3. [Cp*Rh(S=PPh$_2$Py)Cl]PF$_6$ (3). Color: red orange precipitate; yield: 56 mg (79%); IR (KBr, cm^{-1}): 3133(b), 1619(w), 1585(m), 1437(m), 1401(s), 1312(w), 1279(m), 1185 (w), 1159(m), 1131(m), 1101(s), 1019(s), 998(m), 840(vs), 766(s), 709(s), 693(s), 622(m), 606(s), 558(vs), 525(s), 504(s); ^{1}H NMR (400 MHz, CD$_3$CN): δ = 9.02 (d, 1H, H$_{JJ}$ = 3.25, py ring), 8.12 (t, 1H, py ring), 7.88 (d, 2H, H$_{JJ}$ = 2.00, ph ring), 7.79–7.74 (m, 5H, ph ring), 7.60–7.55 (m, 4H, ph ring), 7.43 (t, 1H, py ring), 1.44 (s, 15H, Cp* ring); ^{13}C NMR (400 MHz, CD$_3$CN): δ = 156.73, 153.79, 139.67, 134.16, 132.54, 132.11, 131.32, 129.39, 126.12, 97.63, 7.85; ESI-MS: 568.00 [M$^+$] peak, 532.05 [M$^+$–Cl] peak, 236.05 [Cp*RhCl$^+$] peak; UV–vis {CH$_3$CN, λ_{max} nm (ε, M^{-1} cm^{-1})}: 243(3100), 402(300); Anal. Calcd for C$_{27}$H$_{30}$NSRhClPF$_6$ (714.90) (%): C, 45.36; H, 4.23; N, 1.96. Found (%): C, 45.50; H, 4.42; N, 2.13.

2.3.4. [Cp*Ir(S = PPh₂Py)Cl]PF₆ (4). Color: yellow precipitate; yield: 61 mg (75%); IR (KBr, cm⁻¹): 3436(b), 3094(w), 2994(w), 2925(w), 1585(w), 1455(w), 1439(m), 1384(m), 1313(w), 1187(w), 1136(m), 1100(s), 1027(s), 999(w), 862(s), 841(vs), 781(m), 756(m), 710(m), 626(m), 607(m), 558(s), 523(s), 516(s); ¹H NMR (400 MHz, CD₃CN): 9.14 (d, 1H, H_{JJ} = 3.25, py ring), 8.09 (t, 1H, py ring), 7.84 (d, 2H, H_{JJ} = 2.00, ph ring), 7.67–7.60 (m, 5H, ph ring), 7.56–7.50 (m, 4H, ph ring), 7.39 (t, 1H, py ring), 1.46 (s, 15H, Cp* ring); ¹³C NMR (400 MHz, CD₃CN): δ = 157.82, 154.25, 139.78, 134.38, 132.91, 132.48, 131.79, 129.65, 126.43, 97.65, 8.35; ESI-MS: 658.09 [M⁺] peak, 622.10 [M⁺–Cl] peak, 363.02 [Cp*IrCl⁺] peak; UV–vis {CH₃CN, λ_{max} nm (ε, M⁻¹ cm⁻¹)}: 226(10,000), 314 (2400), 375(900); Anal. Calcd for $C_{27}H_{30}NSIrClPF_6$ (804.21) (%): C, 40.32; H, 3.76; N, 1.74. Found (%): C, 40.51; H, 3.87; N, 1.91.

2.3.5. [(Benzene)Ru(Se = PPh₂Py)Cl]PF₆ (5). Color: orange precipitate; yield: 53 mg (75%); IR (KBr, cm⁻¹): 3431(b), 3133(w), 1637(m), 1587(m), 1479(w), 1436(m), 1400(vs), 1314(w), 1286(m), 1186(w), 1141(m), 1096(s), 1000(w), 836(vs), 771(m), 754(m), 716(m), 688(m), 616(w), 557(vs), 510(s); ¹H NMR (400 MHz, CD₃CN): δ = 9.10 (d, 1H, H_{JJ} = 3.25, py ring), 8.20 (t, 1H, py ring), 7.92 (d, 2H, H_{JJ} = 2.00, ph ring), 7.80–7.75 (m, 5H, ph ring), 7.63–7.57 (m, 4H, ph ring), 7.41 (t, 1H, py ring), 5.60 (s, 6H, benzene ring); ¹³C NMR (400 MHz, CD₃CN): δ = 162.54, 152.20, 136.26, 135.42, 132.67, 131.87, 130.42, 128.62, 126.71, 85.90; ESI-MS: 557.89 [M⁺] peak, 522.90 [M⁺–Cl] peak, 214.90 [(ben)RuCl⁺] peak; UV–vis {CH₃CN, λ_{max} nm (ε, M⁻¹ cm⁻¹)}: 228(7300), 324(700); Anal. Calcd for $C_{23}H_{20}NSeRuClPF_6$ (701.83) (%): C, 39.36; H, 2.87; N, 2.00. Found (%): C, 39.53; H, 2.99; N, 2.17.

2.3.6. [(p-Cymene)Ru(Se=PPh₂Py)Cl]PF₆ (6). Color: orange precipitate; yield: 59 mg (78%); IR (KBr, cm⁻¹): 3434(m), 3129(m), 2970(m), 1631(m), 1584(w), 1456(m), 1439(s), 1400(s), 1320(m), 1280(w), 1186(w), 1133(m), 1100(s), 1054(m), 1028(w), 838(vs), 779 (w), 756(w), 693(m), 557(vs), 518(s); ¹H NMR (400 MHz, CD₃CN): δ = 9.15 (d, 1H, H_{JJ} = 3.25, py ring), 8.21 (t, 1H, py ring), 7.80 (d, 2H, H_{JJ} = 2.25, ph ring), 7.76–7.71 (m, 5H, ph ring), 7.61–7.55 (m, 4H, ph ring), 7.42 (t, 1H, py ring), 5.97 (d, 2H, H_{JJ} = 3.75, ph ring), 5.72 (d, 2H, H_{JJ} = 3.75, ph ring), 2.90 (sep, 1H, Ar$_{(p-Cy)}$), 2.51 (s, 3H, CH₃), 2.01 (s, 3H, CH₃Ar$_{(p-Cy)}$), 1.34 (d, 6H, H_{JJ} = 4.00, CH₃Ar$_{(p-Cy)}$), 1.22 (d, 6H, H_{JJ} = 4.25, CH₃Ar$_{(p-Cy)}$); ¹³C NMR (400 MHz, CD₃CN): δ = 160.26, 153.42, 138.21, 135.71, 132.90, 132.02, 130.65, 129.47, 128.82, 102.73, 90.82, 85.34, 82.51, 31.26, 21.12, 16.54; ESI-MS: 613.93 [M⁺] peak, 578.98 [M⁺–Cl] peak, 236.08 [(p-cy)RuCl⁺] peak; UV–vis {CH₃CN, λ_{max} nm (ε, M⁻¹ cm⁻¹)}: 227(5800), 330(400); Anal. Calcd for $C_{27}H_{28}NSeRuClPF_6$ (757.94) (%): C, 42.79; H, 3.72; N, 1.85. Found (%): C, 42.98; H, 3.86; N, 1.96.

2.3.7. [Cp*Rh(Se=PPh₂Py)Cl]PF₆ (7). Color: red orange precipitate; yield: 61 mg (81%); IR (KBr, cm⁻¹): 3436(b), 2926(w), 1636(m), 1439(m), 1400(m), 1385(w), 1163(m), 1131 (m), 1096(s), 1024(m), 998(w), 861(s), 841(vs), 781(w), 756(m), 716(w), 697(m), 556(vs), 513(s); ¹H NMR (400 MHz, CD₃CN): δ = 9.09 (d, 1H, H_{JJ} = 3.25, py ring), 8.10 (t, 1H, py ring), 7.70 (d, 2H, H_{JJ} = 2.00, ph ring), 7.86–7.74 (m, 5H, ph ring), 7.60–7.52 (m, 4H, ph ring), 7.37 (t, 1H, py ring), 1.42 (s, 15H, Cp* ring); ¹³C NMR (400 MHz, CD₃CN): δ = 158.24, 154.63, 138.95, 134.69, 132.98, 132.25, 130.93, 129.54, 127.02, 97.89, 7.65; ESI-MS: 568.02 [M⁺] peak, 536.01 [M⁺–Se] peak, 236.09 [Cp*RhCl⁺] peak; UV–vis

{CH$_3$CN, λ_{max} nm (ε, M^{-1} cm^{-1})}: 249(4500), 414(400); Anal. Calcd for C$_{27}$H$_{30}$NSeRhClPF$_6$ (761.79) (%): C, 42.57; H, 3.97; N, 1.84. Found (%): C, 42.76; H, 4.08; N, 1.93.

2.3.8. [Cp*Ir(Se = PPh$_2$Py)Cl]PF$_6$ (8). Color: yellow precipitate; yield: 67 mg (65%); IR (KBr, cm^{-1}): 3436(b), 2924(w), 1624(w), 1455(m), 1439(m), 1384(m), 1133(w), 1099(s), 1033(m), 998(w), 862(s), 841(vs), 782(m), 755(m), 731(w), 715(w), 691(m), 556(s), 512 (s); ^{1}H NMR (400 MHz, CD$_3$CN): $\delta = 9.03$ (d, 1H, H$_{JJ}$ = 3.25, py ring), 8.15 (t, 1H, py ring), 7.88 (d, 2H, H$_{JJ}$ = 2.50, ph ring), 7.79–7.60 (m, 5H, ph ring), 7.59–7.55 (m, 4H, ph ring), 7.43 (t, 1H, py ring), 1.43 (s, 15H, Cp* ring); ^{13}C NMR (400 MHz, CD$_3$CN): $\delta = 158.24$, 153.92, 138.86, 135.23, 132.76, 132.89, 131.64, 129.72, 126.61, 97.72, 8.29; ESI-MS: 706.04 [M$^+$] peak, 626.08 [M$^+$–Se] peak, 363.07 [Cp*IrCl$^+$] peak; UV–vis {CH$_3$CN, λ_{max} nm (ε, M^{-1} cm^{-1})}: 226(7600), 307(1300), 386(400); Anal. Calcd for C$_{27}$H$_{30}$NSeIrClPF$_6$ (851.10) (%): C, 38.10; H, 3.55; N, 1.65. Found (%): C, 38.26; H, 3.62; N, 1.78.

2.4. *Syntheses of metal complexes (9)–(12)*

[(Arene)RuCl$_2$]$_2$ or [Cp*MCl$_2$]$_2$ (0.1 mmol), Ph$_2$PyP=O (0.2 mmol), and NH$_4$PF$_6$ (2 M equivalent) were stirred for 4 h in methanol. The yellow solution was evaporated under reduced pressure. The yellow residue was dissolved in dichloromethane and filtered. The filtrate was concentrated to 2 mL and an excess of hexane was added for precipitation. The yellow product was washed with diethylether and dried under vacuum. Spectroscopic data of **9–12** were in agreement with the previously reported complexes [19].

3. Results and discussion

3.1. *Synthesis of the complexes*

The chalcogenide ligands E=PPh$_2$Py {E = S (**L2**); Se (**L3**)} are prepared by direct oxidation using S/Se powder of 2-pyridyldiphenylphosphine (**L1**) in toluene. After evaporation of solvent, crystalline solids are being formed directly from the reaction mixture. The reaction of [(arene)RuCl$_2$]$_2$ {arene = benzene; *p*-cymene} and [Cp*MCl$_2$]$_2$ (M = Rh, Ir) with 2 M equivalents of E=PPh$_2$Py (E = S, Se) afford mononuclear cationic complexes, [(arene)Ru (κ^2-(*NE*)-PPh$_2$Py)Cl]$^+$ and [Cp*M(κ^2-(*NE*)-PPh$_2$Py)Cl]$^+$, in methanol (scheme 1). These complexes are isolated in very good yield by using PF$_6^-$ as counterion and purified by recrystallization. All these complexes are obtained as yellow–orange crystalline non-hygroscopic, air-stable solids. They are highly soluble in acetone, acetonitrile, and DMSO but are sparingly soluble in methanol, dichloromethane, and chloroform. All these complexes are fully characterized by IR, ^{1}H NMR, mass, and electronic spectroscopy.

Preparation of O=PPh$_2$Py (**L4**) is done by the addition of excess aqueous H$_2$O$_2$ (30%) to a THF solution of the PPh$_2$Py as per the reported procedure [4, 6]. We expected the formation of [(arene)Ru(κ^2-(*NO*)-PPh$_2$Py)Cl]$^+$ and [Cp*M(κ^2-(*NO*)-PPh$_2$Py)Cl]$^+$ complexes when reacted with [(arene)RuCl$_2$]$_2$ {M = Ru, arene = benzene; *p*-cymene} and [Cp*MCl$_2$]$_2$ (M = Rh, Ir). Instead, [(arene)Ru(κ^2-(*PN*)-PPh$_2$Py)Cl]$^+$ and [Cp*M(κ^2-(*PN*)-PPh$_2$Py)Cl]$^+$ have been isolated as an unexpected product and the formation of complexes is
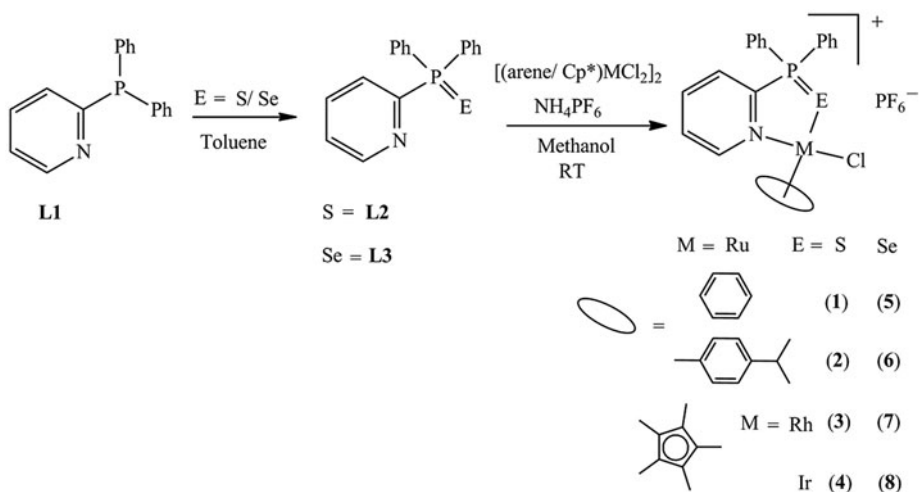
Scheme 1.   Preparation of metal complexes with E=PPh$_2$Py.

unambiguous. It could be deoxygenation of Ph$_2$PyP=O with emphasis on the reductive cleavage of P=O bonds, while the relatively weaker P=S and P=Se bonds are stable under similar reaction environment. Our group has already reported a series of arene Ru and Cp*Rh/Cp*Ir complexes containing PPh$_2$Py by direct reaction. The dinuclear complexes [(arene)RuCl$_2$]$_2$ {M = Ru, arene = benzene; p-cymene} and [Cp*MCl$_2$]$_2$ (M = Rh, Ir) undergo bridge cleavage reaction with PPh$_2$Py yielding cationic P,N-chelating complexes. All these complexes are well studied by spectroscopic techniques [11–13], but the crystal structures of **9** and **12** are not published before; so we present them here to establish the structure and composition of the molecules (scheme 2).
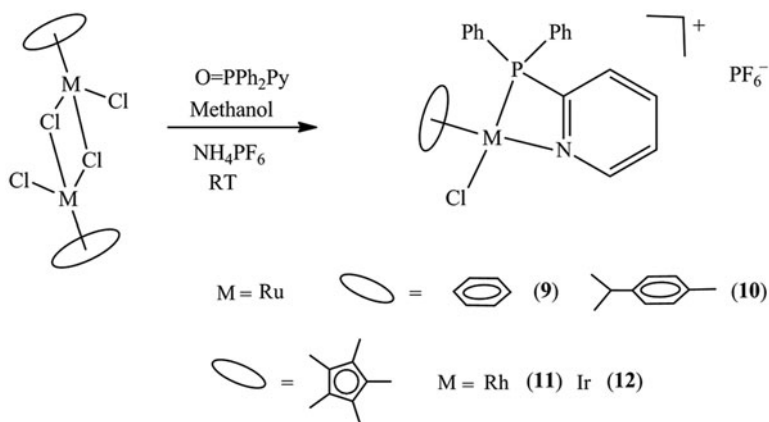
Scheme 2.   Preparation of metal complexes with O=PPh$_2$Py.

3.2. *IR studies of the complexes*

IR spectra of the mononuclear complexes exhibit strong bands around 1580 and 1455 cm^{-1}, corresponding to the stretching frequencies of C=C and C=N of phenyl and pyridine rings of the chalcogenide ligand, respectively. P=E bond stretching frequencies of the metal complexes show a strong band at 625 and 520 cm^{-1} for P=S, P=Se, respectively, in the lower frequency region when free ligand shows these bands at 645 and 567 cm^{-1} [20]. Besides these signals, all the complexes have sharp bands at 841 and 558 cm^{-1}, which correspond to P–F stretching frequency of the counterion [21].

3.3. *NMR studies of the complexes*

^{1}H NMR spectra of all metal complexes exhibit three resonances for protons of the pyridyl ring at 9.38, 7.70, and 7.10 ppm, whereas diphenyl protons exhibit two multiplets at 7.80–7.70 and 7.60–7.50 ppm, similar to the pattern of free ligand except these signals are shifted downfield [22]. Complexes **1** and **5** display a singlet at 6.35 ppm for protons of the arene ligand. Complexes **2** and **6** show two doublets at 6.30 and 6.02 ppm which correspond to the aromatic *p*-cymene ring CH protons, septet at 3.04 ppm as well as a doublet at 1.35 ppm for protons of the isopropyl group, and a singlet at 2.04 ppm for methyl proton of *p*-cymene. The Cp*Rh complexes (**3** and **7**) and Cp*Ir complexes (**4** and **8**) display a singlet at 1.75 and 1.76 ppm due to the Cp* ligand, which is slightly downfield in comparison to the starting materials. Due to ligand coordinated, the signals are shifted to downfield compared to free ligand, which indicates the formation of mononuclear complexes [23].

^{13}C NMR spectra also show signals expected for metal coordinated arene/Cp* groups and the E=PPh$_2$Py ligand. All complexes exhibit nine clusters of peaks from 160.10 to 126.25 ppm for pyridyl and phenyl ring carbons of ligand. The arene ruthenium complexes (**1** and **5**) display a peak at 120 ppm and **2** and **6** display seven peaks from 100 to 115 ppm, which is typical for arene ligand. Complexes **3**, **4**, **7**, and **8** show a sharp singlet at
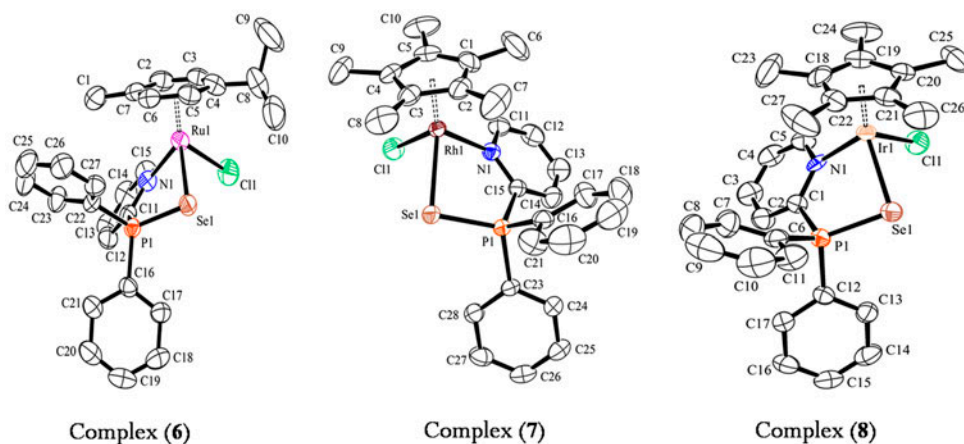

Figure 2. Molecular structures of [(*p*-cymene)Ru(Se=PPh$_2$Py)Cl]PF$_6$ (**6**), [Cp*Rh(Se=PPh$_2$Py)Cl]PF$_6$ (**7**), and [Cp*Ir(S=PPh$_2$Py)Cl]PF$_6$ (**8**) with 50% probability thermal ellipsoids. Counterion and hydrogens are omitted for clarity.

8.50 ppm that correspond to Cp* methyl carbon, signals are shifted downfield compared to the metal precursor and free ligand which indicates formation of metal complexes [24].

3.4. *Mass studies of the complexes*

Mass spectral analyses have been recorded in CH_3CN and *m/z* values are listed in the Section 2. The mass spectra of all complexes display prominent peaks corresponding to the molecular ion fragment, in agreement with the theoretically expected values. In ESI spectra, parent peaks have been found (*m/z*) from thio metal complexes at 509.90 (**1**), 566.10 (**2**), 568.00 (**3**), 658.90 (**4**) and seleno metal complexes at 557.89 (**5**), 613.93 (**6**), 615.90 (**7**), and 706.04 (**8**). These signals show loss of chloride ions from molecular ion peak. All the complexes show $[(arene/Cp*)MCl^+]$ ion fragment, which indicates stronger bond between the metal ion and arene ligand [25].

3.5. *Molecular structural studies*

The molecular structures of the complexes have been determined by single-crystal X-ray analysis. ORTEP diagrams of the complexes are shown in figures 1–3. Crystallographic and structure refinement parameters are given in table 1. Selected bond lengths and angles are presented in table 2. Complexes **2**–**8** show a typical three-legged piano stool structure with the metal center coordinated by chloride and the chelating ligand in k^2-N,S/Se mode as the legs and the η^6-arene/Cp* ligand occupying three facial coordinations (figures 1 and 2). The metal has pseudo-octahedral arrangement and with formation of a five-membered metallacycle. Hexafluorophosphate is the counterion in all the complexes. The complexes have normal bond distances and angles but slightly vary in bond distances and bond angles between sulfur and selenium ligand to the metal. The average metal to carbon and centroid of the arene/Cp* ring distances in all complexes are 2.158(4)–2.196(4) Å and
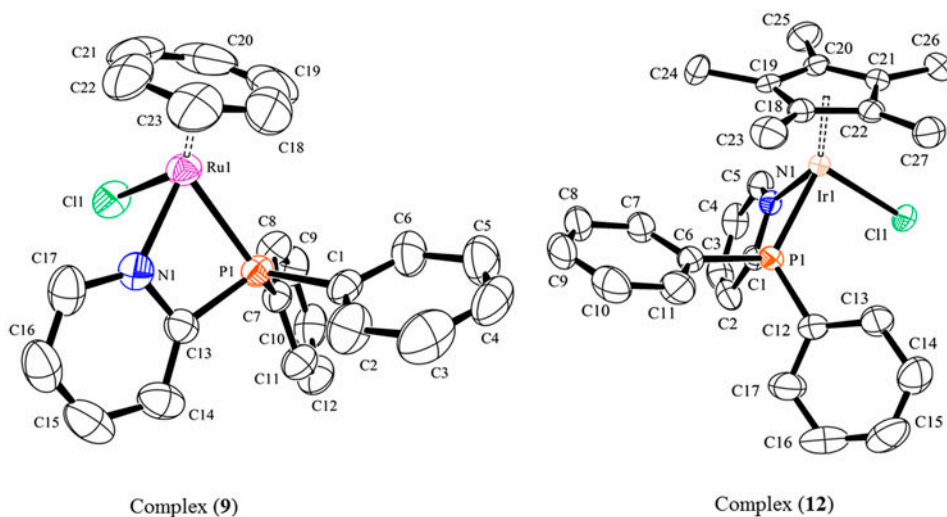

Complex (9)   Complex (12)

Figure 3. Molecular structures of [(benzene)Ru(PPh₂Py)Cl]PF₆ (**9**) and [Cp*Ir(PPh₂Py)Cl]PF₆ (**12**) with 50% probability thermal ellipsoids. Counterion, hydrogens, and solvent molecule are omitted for clarity.
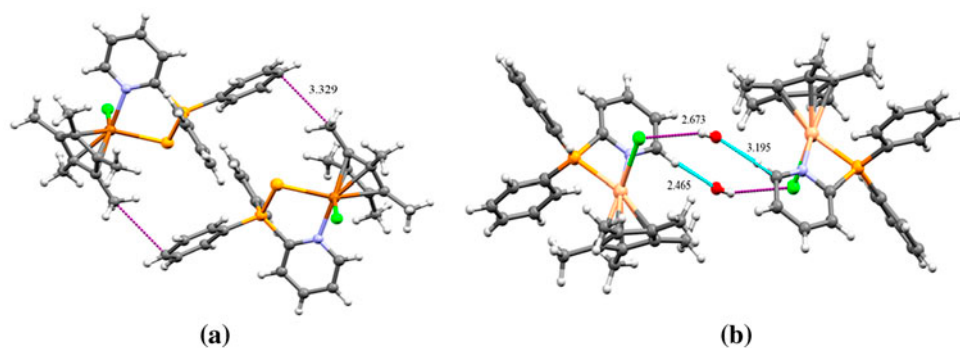
Figure 4.   (a) View of **7** showing the dimeric pair of π–π interaction; (b) view of **12** showing the dimeric pair of O–H–Cl interaction and C–H–O interaction along with water molecule.

1.677–1.796 Å. The metal to chloride and metal to nitrogen bond distances are 2.3815(12)–2.4034(17) Å and 2.123(3)–2.109(5) Å, respectively, which are almost identical to earlier reported values [26–28].

The metal to sulfur bond length of **2** is 2.3729(14) Å, that is, close to reported values [(arene)Ru(NS)Cl]$^+$ {where NS is (2-arylthio-methyl)pyridine 2.3771(18)–2.374(9) Å [29]; N-[2-(arylthio)-ethyl]morpholine 2.3742(14)–2.3815(12) Å [30]; 1-pyrimidyl-3-methyl-imidazoyl-2-thione 2.3933(9) Å [31]}. The metal to selenium bond lengths of complexes are 2.5185(5) Å (**6**), 2.5201(5) Å (**7**), and 2.5189(7) Å (**8**), longer than [(arene/Cp*)M(NSe)Cl]$^+$ {where NSe is (2-arylseleno-methyl)pyridine 2.4879(7) Å [29]; N-[2-(arylseleno)ethyl]-morpholine 2.4837(14) Å [30]} and smaller than {6-selenopurine and 6-selenogua-nine 2.5337(8)–2.5574(9) Å [32]} and [(arene/Cp*)M(Se∩Se)Cl]$^+$ {where Se∩Se is 1,2-bis(phenylseleno)ethane 2.4579(13)–2.4864(12) Å [33]; bis(diphenylphosphino)amino-dichalcogenide 2.5266(8)–2.5361(11) Å [34]} in which such a bond length is close to the reported values. In all the complexes, the P=S/Se bond distances are longer than that of the free ligand, but the C–N bond distances of the complexes are slightly elongated on coordination. The bite angle N–M–S/Se and bond angles N–M–Cl and S/Se–M–Cl are close to 90°. These bond distances and various bond angles support piano stool geometry about the metal center and are in agreement with the values reported in the literature of other closely related complexes [25, 35, 36]. In all the complexes, a number of interesting weak interactions like C–H···Cl and π···π interactions have been observed in the solid-state packing which play a vital role in the building of supramolecular motifs and dominant role in stabilizing the stacking of molecules [37–39]. For example, **7** assembles the inverted piano stool dimeric complex formed by weak interaction of C–H…π contact between the Cp* CHs and diphenyl ligand with distance 3.329 Å [figure 4(a)].

Complexes **9** and **12** are expected to have a three-legged pseudo-octahedral piano stool structure with the chelating derivative ligand in k^2-PN mode in a four-membered metallacycle (figure 3). X-ray crystallography of these complexes show no significant difference in bond distances and lengths, related to previous reported half-sandwich arene Ru complexes with 2-pyridyldiphenylphosphine [12, 13, 16]. Complex **12** crystallizes with one water in a cen-trosymmetric supramolecular dimer. Two water molecules bridge two molecules of metal bound chloride and pyridyl ring pair related via weak interaction of O–H…Cl, O…C–H/O…H–C contacts with bond distances 2.673, 3.195, and 2.465 Å, giving a $R_4^4(12)$ metallorganic dimeric unit [figure 4(b)] [40].

3.6. *UV–vis studies of the complexes*

UV–visible spectra of the complexes were recorded in acetonitrile ~10^{-4} M concentration solution from 200 to 550 nm. All the complexes show intense absorption at 226–335 nm, assigned to π–π*/n–π* transition. Low intensity band at 375–420 nm corresponds to metal ligand charge transfer transition, from excitation of electrons from the metal t_{2g} level to the π* orbitals of the ligands [41].

4. Conclusion

Cationic arene Ru and Cp*Rh/Cp*Ir complexes containing chalcogenide derivative ligands E=PPh$_2$Py (E=S, Se) have been synthesized and characterized. X-ray crystallographic analysis confirmed that the complexes have three-legged piano stool geometries. Solid-state structure of complexes show weak interactions like O–H···Cl, C–H···π and π···π short contacts which play an essential role in stabilizing the stacking of molecules.

Supplementary material

CCDC-1050876 (**2**), 1050877 (**6**), 1050878 (**7**), 1050879 (**8**), 1050874 (**9**), and 1050875 (**12**) contain the supplementary crystallographic data for this paper. These data can be obtained free of charge via www.ccdc.cam.ac.uk/data_request/cif, by emailing data_request@ccdc.cam.ac.uk, or by contacting the Cambridge Crystallographic Data Center, 12 Union Road, Cambridge CB2 1EZ, UK; Fax: +44 1223 336033.

Disclosure statement

No potential conflict of interest was reported by the authors.

Supplemental data

Supplemental data for this article can be accessed at http://dx.doi.org/10.1080/00958972.2015.1087514.

References

[1] P. Espinet, K. Soulantica. *Coord. Chem. Rev.*, **193–195**, 499 (1999).
[2] C. Khin, A. Hashmi, F. Rominger, F. Rominger. *Eur. J. Inorg. Chem.*, **7**, 1063 (2010).
[3] P. Kumar, A.K. Singh, S. Sharma, D.S. Pandey. *J. Organomet. Chem.*, **694**, 3643 (2009).
[4] P.K. Majhi, G. Schnakenburg, R. Streubel. *Dalton Trans.*, **43**, 16673 (2014).
[5] R. Sevcik, M. Necas, J. Novosad. *Polyhedron*, **22**, 1585 (2003).
[6] W. Lackner-Warton, S. Tanaka, C.M. Standfest-Hauser, Ö. Öztopcu, J.C. Hsieh, K. Mereiter, K. Kirchner. *Polyhedron*, **29**, 3097 (2010).
[7] G.P. Suranna, P. Mastrorilli, C.F. Nobile, W. Keim. *Inorg. Chim. Acta*, **305**, 151 (2000).
[8] D. Cauzzi, C. Graiff, C. Massera, G. Predieri. *Eur. J. Inorg. Chem.*, **3**, 721 (2001).
[9] P. Das, D. Konwar, P. Sengupta, D.K. Dutta. *Transition Met. Chem.*, **25**, 426 (2000).
[10] D.K. Dutta, B. Deb. *Coord. Chem. Rev.*, **255**, 1686 (2011).
[11] R. Lalrempuia, P.J. Carroll, M.R. Kollipara. *J. Coord. Chem.*, **56**, 1499 (2003).
[12] R. Lalrempuia, P.J. Carroll, M.R. Kollipara. *J. Chem. Sci.*, **116**, 21 (2004).
[13] P. Govindaswamy, Y.A. Mozharivskyj, M.R. Kollipara. *Polyhedron*, **23**, 3115 (2004).
[14] D.D. Perrin, W.L.F. Armarego. *Purification of Laboratory Chemicals*, 4th Edn, p. 416, Butterworths Heinemann, London (1996).
[15] J. Tönnemann, J. Risse, Z. Grote, R. Scopelliti, K. Severin. *Eur. J. Inorg. Chem.*, **26**, 4558 (2013).
[16] G.M. Sheldrick. *Acta Cryst.*, **A46**, 467 (1990).
[17] G.M. Sheldrick. *SHELXS-97 and SHELXL-97*, University of Gottingen, Gottingen, Germany (1999).
[18] WinGX, L.J. Farrugia. *J. Appl. Crystallogr.*, **32**, 837 (1999).
[19] R.G. Alvarez, S.E.G. Garrido, J. Díez, P. Crochet, V. Cadierno. *Eur. J. Inorg. Chem.*, **26**, 4218 (2012).
[20] H. Christina, E. McFarlane, W. McFarlane, A.S. Muir. *Polyhedron*, **9**, 1757 (1990).
[21] K. Nakamoto, *Infrared and Raman Spectra of Inorganic and Coordination Complexes*, Part A, 6th Edn, p. 221, John Wiley & Sons, Inc., Hoboken, NJ (2009).
[22] K.W. Hermanowicz, Z. Ciunik, A. Kochel. *Inorg. Chem.*, **45**, 3369 (2006).
[23] D. Drommi, C.G. Arena, F. Nicolo, G. Bruno, F. Faraone. *J. Organomet. Chem.*, **485**, l15 (1995).
[24] R.G. Alvarez, J. Díez, P. Crochet, V. Cadierno. *Organometallics*, **29**, 3955 (2010).
[25] K. Mahesh, S.H. Forbes, Y. Mozharivskyj, K.M. Rao. *Inorg. Chim. Acta*, **421**, 218 (2014).
[26] H. Mishra, R. Mukherjee. *J. Organomet. Chem.*, **695**, 1753 (2010).
[27] G. Gupta, K.T. Prasad, B. Das, G.P.A. Yap, K.M. Rao. *J. Organomet. Chem.*, **694**, 2618 (2009).
[28] M.U. Raja, J. Tauchman, B. Therrien, G. Süss-Fink, T. Riedel, P.J. Dyson. *Inorg. Chim. Acta*, **409**, 479 (2014).
[29] O. Prakash, K.N. Sharma, H. Joshi, P.L. Gupta, A.K. Singh. *Dalton Trans.*, **42**, 8736 (2013).
[30] P. Singh, A.K. Singh. *Eur. J. Inorg. Chem.*, **26**, 4187 (2010).
[31] V.A. Rao, R. Pallepogu, Z.Y. Zhou, K.M. Rao. *Inorg. Chim. Acta*, **387**, 37 (2012).
[32] R. Mitra, A.K. Pramanik, A.G. Samuelson. *Eur. J. Inorg. Chem.*, **33**, 5733 (2014).
[33] O. Prakash, K.N. Sharma, H. Joshi, P.L. Gupta, A.K. Singh. *Organometallics*, **33**, 983 (2014).
[34] M. Valderrama, R. Contreras, M.P. Lamata, F. Viguri, D. Carmona, F.J. Lahoz, S. Elipe, L.A. Oro. *J. Organomet. Chem.*, **607**, 3 (2000).
[35] O. Prakash, P. Singh, G. Mukherjee, A.K. Singh. *Organometallics*, **31**, 3379 (2012).
[36] F. Saleem, G.K. Rao, A. Kumar, G. Mukherjee, A.K. Singh. *Organometallics*, **32**, 3595 (2013).
[37] M. Nishio. *Cryst. Eng. Comm.*, **6**, 130 (2004).
[38] A. Bacchi, G. Cantoni, M. Granelli, S. Mazza, P. Pelagatti, G. Rispoli. *Cryst. Growth Des.*, **11**, 5039 (2011).
[39] B. Cheng, A.A. Tehrani, M.L. Hu, A. Morsali. *Cryst. Eng. Commun.*, **16**, 9125 (2014).
[40] A. Bacchi, G. Cantoni, M.R. Chierotti, A. Girlando, R. Gobetto, G. Lapadula, P. Pelagatti, A. Sironi, M. Zecchini. *Cryst. Eng. Comm.*, **13**, 4365 (2011).
[41] K. Mahesh, R. Nagarajaprakash, S. Forbes, Y. Mozharivskyj, K.M. Rao. *Z. Anorg. Allg. Chem.*, **641**, 715 (2015).